

The fifth column shows  $S_0(A)$ ,  $S_1(A) \oplus B$ , and  $(S_2(A) \oplus 2B) = (S_2(A) \oplus B) \oplus B$ . Finally, the last column shows reconstruction of set  $A$ , which, according to Eq. (9.5-15), is the union of the dilated skeleton subsets shown in the fifth column. ■

### 9.5.8 Pruning

Pruning methods are an essential complement to thinning and skeletonizing algorithms because these procedures tend to leave parasitic components that need to be “cleaned up” by postprocessing. We begin the discussion with a pruning problem and then develop a morphological solution based on the material introduced in the preceding sections. Thus, we take this opportunity to illustrate how to go about solving a problem by combining several of the techniques discussed up to this point.

A common approach in the automated recognition of hand-printed characters is to analyze the shape of the skeleton of each character. These skeletons often are characterized by “spurs” (parasitic components). Spurs are caused during erosion by non uniformities in the strokes composing the characters. We develop a morphological technique for handling this problem, starting with the assumption that the length of a parasitic component does not exceed a specified number of pixels.

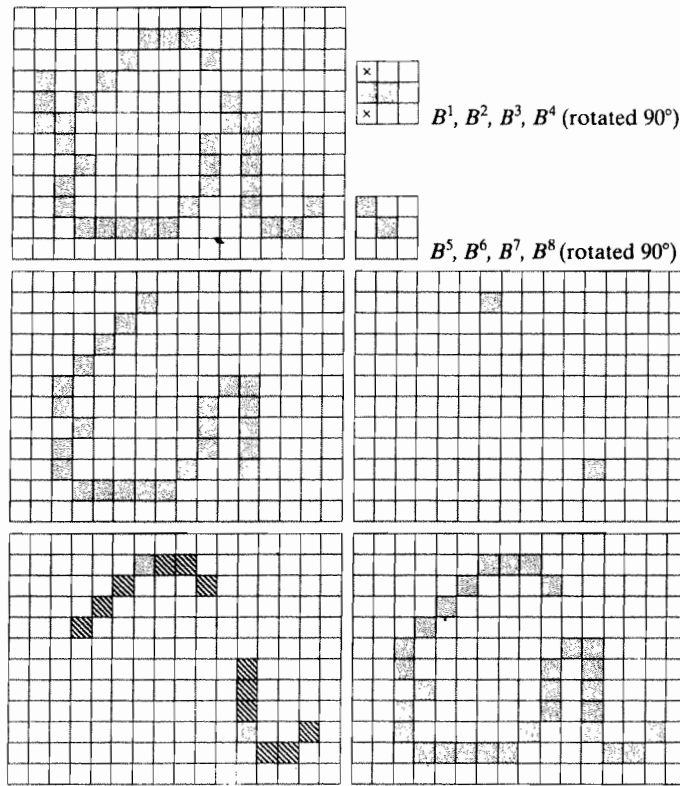
Figure 9.25(a) shows the skeleton of a hand-printed “a.” The parasitic component on the leftmost part of the character is illustrative of what we are interested in removing. The solution is based on suppressing a parasitic branch by successively eliminating its end point. Of course, this also shortens (or eliminates) other branches in the character but, in the absence of other structural information, the assumption in this example is that any branch with three or less pixels is to be eliminated. Thinning of an input set  $A$  with a sequence of structuring elements designed to detect only end points achieves the desired result. That is, let

$$X_1 = A \otimes \{B\} \quad (9.5-17)$$

where  $\{B\}$  denotes the structuring element sequence shown in Figs. 9.25(b) and (c) [see Eq. (9.5-7) regarding structuring-element sequences]. The sequence of structuring elements consists of two different structures, each of which is rotated  $90^\circ$  for a total of eight elements. The  $\times$  in Fig. 9.25(b) signifies a “don’t care” condition, in the sense that it does not matter whether the pixel in that location has a value of 0 or 1. Numerous results reported in the literature on morphology are based on the use of a *single* structuring element, similar to the one in Fig. 9.25(b), but having “don’t care” conditions along the entire first column. This is incorrect. For example, this element would identify the point located in the eighth row, fourth column of Fig. 9.25(a) as an end point, thus eliminating it and breaking connectivity in the stroke.

Applying Eq. (9.5-17) to  $A$  three times yields the set  $X_1$  in Fig. 9.25(d). The next step is to “restore” the character to its original form, but with the parasitic

We may define an *end point* as the center point of a  $3 \times 3$  region that satisfies any of the arrangements in Figs. 9.25(b) or (c).



a b  
c  
d e  
f g

**FIGURE 9.25**

(a) Original image. (b) and (c) Structuring elements used for deleting end points. (d) Result of three cycles of thinning. (e) End points of (d). (f) Dilation of end points conditioned on (a). (g) Pruned image.

branches removed. To do so first requires forming a set  $X_2$  containing all end points in  $X_1$  [Fig. 9.25(e)]:

$$X_2 = \bigcup_{k=1}^8 (X_1 \otimes B^k) \quad (9.5-18)$$

where the  $B^k$  are the same end-point detectors shown in Figs. 9.25(b) and (c). The next step is dilation of the end points three times, using set  $A$  as a delimiter:

$$X_3 = (X_2 \oplus H) \cap A \quad (9.5-19)$$

where  $H$  is a  $3 \times 3$  structuring element of 1s and the intersection with  $A$  is applied after each step. As in the case of region filling and extraction of connected components, this type of conditional dilation prevents the creation of 1-valued elements outside the region of interest, as evidenced by the result shown in Fig. 9.25(f). Finally, the union of  $X_3$  and  $X_1$  yields the desired result,

$$X_4 = X_1 \cup X_3 \quad (9.5-20)$$

in Fig. 9.25(g).

In more complex scenarios, use of Eq. (9.5-19) sometimes picks up the "tips" of some parasitic branches. This condition can occur when the end

Equation (9.5-19) is the basis for morphological reconstruction by dilation, as explained in the next section.

points of these branches are near the skeleton. Although Eq. (9.5-17) may eliminate them, they can be picked up again during dilation because they are valid points in  $A$ . Unless entire parasitic elements are picked up again (a rare case if these elements are short with respect to valid strokes), detecting and eliminating them is easy because they are disconnected regions.

A natural thought at this juncture is that there must be easier ways to solve this problem. For example, we could just keep track of all deleted points and simply reconnect the appropriate points to all end points left after application of Eq. (9.5-17). This option is valid, but the advantage of the formulation just presented is that the use of simple morphological constructs solved the entire problem. In practical situations when a set of such tools is available, the advantage is that no new algorithms have to be written. We simply combine the necessary morphological functions into a sequence of operations.

### 9.5.9 Morphological Reconstruction

The morphological concepts discussed thus far involve an image and a structuring element. In this section, we discuss a powerful morphological transformation called *morphological reconstruction* that involves two images and a structuring element. One image, the *marker*, contains the starting points for the transformation. The other image, the *mask*, constrains the transformation. The structuring element is used to define connectivity.<sup>†</sup>

#### Geodesic dilation and erosion

Central to morphological reconstruction are the concepts of geodesic dilation and geodesic erosion. Let  $F$  denote the marker image and  $G$  the mask image. It is assumed in this discussion that both are binary images and that  $F \subseteq G$ . The *geodesic dilation* of size 1 of the marker image with respect to the mask, denoted by  $D_G^{(1)}(F)$ , is defined as

$$D_G^{(1)}(F) = (F \oplus B) \cap G \quad (9.5-21)$$

where  $\cap$  denotes the set intersection (here  $\cap$  may be interpreted as a logical AND because the set intersection and logical AND operations are the same for binary sets). The geodesic dilation of size  $n$  of  $F$  with respect to  $G$  is defined as

$$D_G^{(n)}(F) = D_G^{(1)}[D_G^{(n-1)}(F)] \quad (9.5-22)$$

with  $D_G^{(0)}(F) = F$ . In this recursive expression, the set intersection in Eq. (9.5-21) is performed at each step.<sup>‡</sup> Note that the intersection operator guarantees that

<sup>†</sup>In much of the literature on morphological reconstruction, the structuring element is tacitly assumed to be isotropic and typically is called an *elementary isotropic structuring element*. In the context of this chapter, an example of such an SE is simply a  $3 \times 3$  array of 1s with the origin at the center.

<sup>‡</sup>Although it is more intuitive to develop morphological-reconstruction methods using recursive formulations (as we do here), their practical implementation typically is based on more computationally efficient algorithms (see, for example, Vincent [1993] and Soille [2003]). All image-based examples in this section were generated using such algorithms.